The Depositional Record
The journal of the International Association of Seidmentologisits
Open Access

ORIGINAL RESEARCH ARTICLE

Fault-block rotation controlling the distribution of fluvial sediments; a quantitative test on a Lower Pennsylvanian (Carboniferous) cyclothem succession

FRANK J. G. VAN DEN BELT*, POPPE L. DE BOER* and FRANK VAN BERGEN†,[1]

*Department of Earth Sciences, University of Utrecht, P.O. Box 80021, 3508 TA, Utrecht, The Netherlands (E-mail: f.j.g.vandenbelt@uu.nl)
†TNO/Geological Survey of the Netherlands, Princetonlaan 6, P.O. Box 80015, 3508 TA, Utrecht, The Netherlands

Keywords
Cyclothems, floodplain, fluvial, Pennsylvanian, subsidence.

[1]Present address: Nexen Petroleum UK Ltd., Prospect House, 97 Oxford Road, Uxbridge UB8 1LU, UK.

Manuscript received: 22 October 2014; Accepted: 25 February 2015

The Depositional Record 2015, 1(1):1–17

doi: 10.1002/dep2.1

ABSTRACT

Depositional models of axial fluvial systems in half-grabens predict that the fluvial-sandstone percentage increases towards the downthrown side of a fault, because channel systems tend to migrate to the area of maximum subsidence. This migration is at the expense of mudstone, but floodplain deposition occurs near faults occasionally. The models assume gradual, transverse tilting and no external base-level change, and their applicability to cases involving tectonics and/or sea-level change may therefore be restricted. Here, a quantitative analysis is presented on a subsurface data set from a Lower Pennsylvanian cyclothem succession, which formed under conditions of differential subsidence and fluctuating sea-level. The studied interval is wedge-shaped and shows a systematic thickness increase from 165 to 245 m, controlled by syndepositional fault-block tilting. It comprises three depositional units, bounded by coal groups. These units display an upward change from wedge-shaped (75 to 120 m) to tabular (42 to 55 m). Despite their variable thickness, the units contain almost equal amounts of *ca* 45 m of floodplain deposits, plus *ca* 5 m of encased channel sandstones, in all boreholes. Where units are thicker, the remaining thickness comprises fluvial-braidplain sandstone. This arrangement indicates that the units represent equal time periods, during which background subsidence allowed the deposition of thin channel sands and overbank mud on a level floodplain. Occasional tilting produced additional accommodation space, which was completely filled by sand-dominated braided systems. The temporary cessation of floodplain-mud deposition suggests that aggradation of the river system could not keep up with floodplain tilting. In addition, bypass of floodplain fines may have been promoted by a basin parallel tilting component. It is shown that (i) cases in which the standard models fully apply, and (ii) cases in which differential subsidence is too strong or too abrupt, can be distinguished by analysing cross-plots of cumulative-sandstone and cumulative-mudstone thickness.

INTRODUCTION

Pennsylvanian (Upper Carboniferous) sedimentary successions in Euramerican basins are characterized by repetitive fluvio-deltaic cycles that formed in response to glacio-eustatic sea-level fluctuations (Davies, 2008; Greb *et al.*, 2008; Rygel *et al.*, 2008). These cycles, also known as 'cyclothems' (Weller, 1930), are a few metres to tens of metres thick and commonly comprise deltaic or marine shales overlain by alternations of fluvial sandstone, floodplain mud and coal-bearing coastal-plain deposits (Fielding, 1984a; Guion *et al.*, 1995). The fluvial sandstones are mostly extensive, erosively based bodies with a thickness up to 15 to 20 m, and their width is estimated to be anywhere between a few and tens of kilometres (Fielding, 1986; Aitken & Flint, 1995; Guion & Rippon, 1995; Rippon, 1996; Jones & Glover, 2005; Rygel *et al.*, 2008).

Synsedimentary tectonics may influence or control the distribution and (stacked) thickness of the fluvial sandstones. In the Pennine Basin (UK) major fluvial-sandstone

bodies appear stacked on hangingwall blocks (Fielding, 1984a, 1986; Fielding & Johnson, 1987; Guion & Fielding, 1988; Rippon, 1996). This arrangement was attributed to the tendency of fluvial channels to seek low-lying areas after avulsion events (cf. Alexander & Leeder, 1987; Leeder & Gawthorpe, 1987). Collinson *et al.* (1993) described comparable sandstone stacking in the Pennsylvanian below the adjacent Southern North Sea. The laterally offset, 'diagonal' stacking of channel bodies observed by Fielding (1984a) was considered evidence of progressive downslope channel migration. In various sub-basins of the Appalachian foreland (USA), similar observations were made. For the Warrior Basin (Alabama), Weisenfluh & Ferm (1984) and Ferm & Weisenfluh (1989) described how a number of *ca* 1 km wide fluvial channels flowed parallel to a major fault on the hangingwall block over a distance of 10 to 15 km, stacking into a 30 m thick compound sandstone unit. Horne (1978) and Allen (1993) observed similar channel-stacking patterns in eastern Kentucky and West Virginia. Also, in those cases, clustering of fluvial-channel sandstone bodies is attributed to the tendency of channels to migrate to low-lying areas at the downthrown side of synsedimentary active faults (Ferm & Weisenfluh, 1989).

The tendency of fluvial channels to preferentially occupy areas of maximum subsidence, and associated sandstone-body stacking near faults, was first described by Alexander & Leeder (1987) and Leeder & Gawthorpe (1987) and has been incorporated in modelling studies since the late 70s. Pioneering theoretical work by Allen (1978) and Bridge & Leeder (1979) was followed by numerous quantitative studies investigating various aspects of alluvial sedimentation (Hajek *et al.*, 2010; Straub *et al.*, 2013; Kopp & Kim, 2015), including the response of fluvial systems to half-graben tilting (Bridge & Mackey, 1993; Mackey & Bridge, 1995; Kim *et al.*, 2010). Here, we refer to these studies collectively as LAB-models (Leeder, Allen and Bridge), following Bryant *et al.* (1995). These theoretical models are supported by a few (semi-)quantitative field tests only (Mack & James, 1993; Leeder *et al.*, 1996; Peakall, 1998) and the rarity of high-quality quantitative data sets has hampered thorough testing of the models (Paola, 2000).

An element of some of the LAB-models is the prediction of the response of fluvial systems to tilting of a floodplain and how this controls alluvial stratigraphy. For example, cross-sections from Bridge & Leeder (1979) and Bridge & Mackey (1993) show slightly different results, but overall the model output displays an increase of cumulative-sandstone thickness (Fig. 1). This increase is non-linear, because at the same time the sandstone percentage increases. Despite the related decrease in the

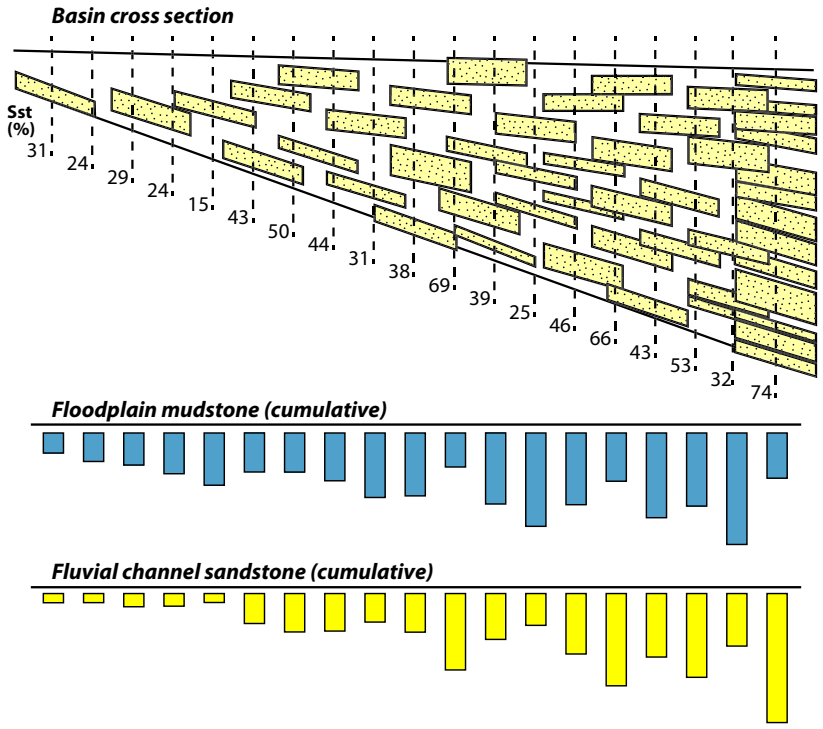

Fig. 1. Half-graben cross-section showing the distribution of fluvial channels (redrawn after Bridge & Mackey, 1993). Sandstone percentage, cumulative-sandstone and cumulative-mudstone thickness are indicated.

mudstone percentage, the predictions show that the cumulative-mudstone thickness does still increase towards the fault.

The LAB-models are based on gradual subsidence and do not account for drastic changes in base level, i.e. due to glacio-eustasy, which may put limitations on their general applicability. Furthermore, the models are based on situations in which a floodplain is tilted exactly perpendicular to the block-margin fault; in actual situations, however, there may be a longitudinal tilting component. Longitudinal tilting has been dealt with in a number of studies (Mackey & Bridge, 1995; Heller & Paola, 1996), although for symmetrical basins only, and it is found to result in downstream changes of alluvial architecture by promoting channel avulsions.

A number of recent studies have pointed out that floodplain tilting does not automatically result in channel migration towards the area of maximum subsidence. Kim *et al.* (2010) have shown, based on laboratory simulations, that axial channels are only forced to migrate towards a fault when lateral channel mobility and/or tilting rates are high. Peakall (1998) has determined for the Holocene Carson River (U.S.A.) that channel systems indeed migrated towards the marginal fault shortly after faulting events, but that they migrated away from the fault during periods of tectonic quiescence. Furthermore, channel systems may be forced to migrate by means of avulsion when the lateral tilt rate is high, or gradually when low (Peakall *et al.*, 2000).

In this paper, results are presented of a detailed quantitative analysis of the control of subsidence on the distribution of fluvial sandstones under strong differential subsidence in a rotational fault-block setting with a fault-parallel tilting component. A three-dimensional borehole data set was analysed, from a Lower Pennsylvanian coal-bearing sequence in a coal-mining concession area in the Upper Silesian Coal Basin (USCB) in Poland (Van Bergen *et al.*, 2006, 2009; Van den Belt, 2012). Only rudimentary sedimentary descriptions were available for the boreholes, which did not allow accurate interpretation of facies. However, a high borehole density in an area of considerable differential subsidence, and a well-established coal-bed framework, makes this an interesting data set to quantitatively test how differential subsidence may control the distribution of fluvial sands.

GEOLOGICAL BACKGROUND

The USCB is a narrow, north–south aligned foreland basin (Fig. 2) in Poland and the Czech Republic (Ziegler, 1990; Zdanowski & Zakowa, 1995). It is bordered by the Moldanubian thrust zone in the west and the East Silesian High in the east, and is strongly asymmetrical. The basement consists of strongly folded metamorphic and plutonic Precambrian and Cambrian rocks. In many parts of the basin, including the study area, the basement is block-faulted, and normal faulting and fault-block rotation associated with this fault system influenced sedimentation during the Devonian (Ziegler, 1990) and Carboniferous (Jureczka & Kotas, 1995). Ziegler (1990) attributed subsidence to tectonic loading of foreland crust and noted that a dextral shear component is required to explain crustal shortening in the Rhenohercynian Basin.

During the Mississippian (Early Carboniferous), the basin was characterized by carbonate-platform deposition throughout, and at the onset of the Namurian deep-water clastics accumulated in the narrow foredeep east of the Moldanubian thrust zone, indicating the onset of regional compression and accelerated subsidence (Zdanowski & Zakowa, 1995). Thrusting started in the Namurian and resulted in a Namurian-Westphalian clastic sediment wedge that thickens westwards (Fig. 2C). In the northwestern part of the basin the stratigraphic column is up to 8·5 km thick locally (Kotas, 1994; Zdanowski & Zakowa, 1995; Doktor, 2007). Alternations of fluvio-deltaic sandstone, mudstone and coal characterize the Namurian-Westphalian succession. Fluvial systems originated in the Moldanubian thrust zone and drained to the north and north-east (Fig. 2C; Kotas, 1994).

The Carboniferous stratigraphy of the basin is illustrated in Fig. 3. The studied interval spans the Upper Silesian Sandstone Series (USSS; Namurian C) and the lower part of the Mudstone Series (Westphalian A-B). The USSS is a fluvial sandstone-rich unit with a thickness of up to 1·1 km close to the thrust zone that rapidly thins eastwards (Kotas, 1994). In the study area, it is between 125 and 200 m thick. It unconformably overlies the mudstone-dominated sediments from the Namurian A (Paralic Series) and across most of the basin, its base is marked by regional coal bed 510. The top of the USSS is a goniatite-bearing 'marine band' that marks the Namurian-Westphalian boundary.

The USSS contains nearly 10% coal and many of the coal beds are between 4 and 8 m thick (Kotas, 1994). The abundance of fluvial-sandstone bodies is attributed to the Late-Namurian 'Erzgebirgian' thrusting event taking place at the western basin margin (Kotas, 1994; Zdanowski & Zakowa, 1995). Sediment sourced from the upthrusted area was transported in an overall north–north-eastward direction by basin-parallel fluvial systems, close to the axis of maximum subsidence (Kotas, 1994; Doktor, 2007). Kotas (1995) reports eastward and north-eastward fluvial transport directions for the USSS.

In the eastern parts of the basin subsidence rates were low during deposition of the USSS, thus shielding the area from sediment input and promoting the formation

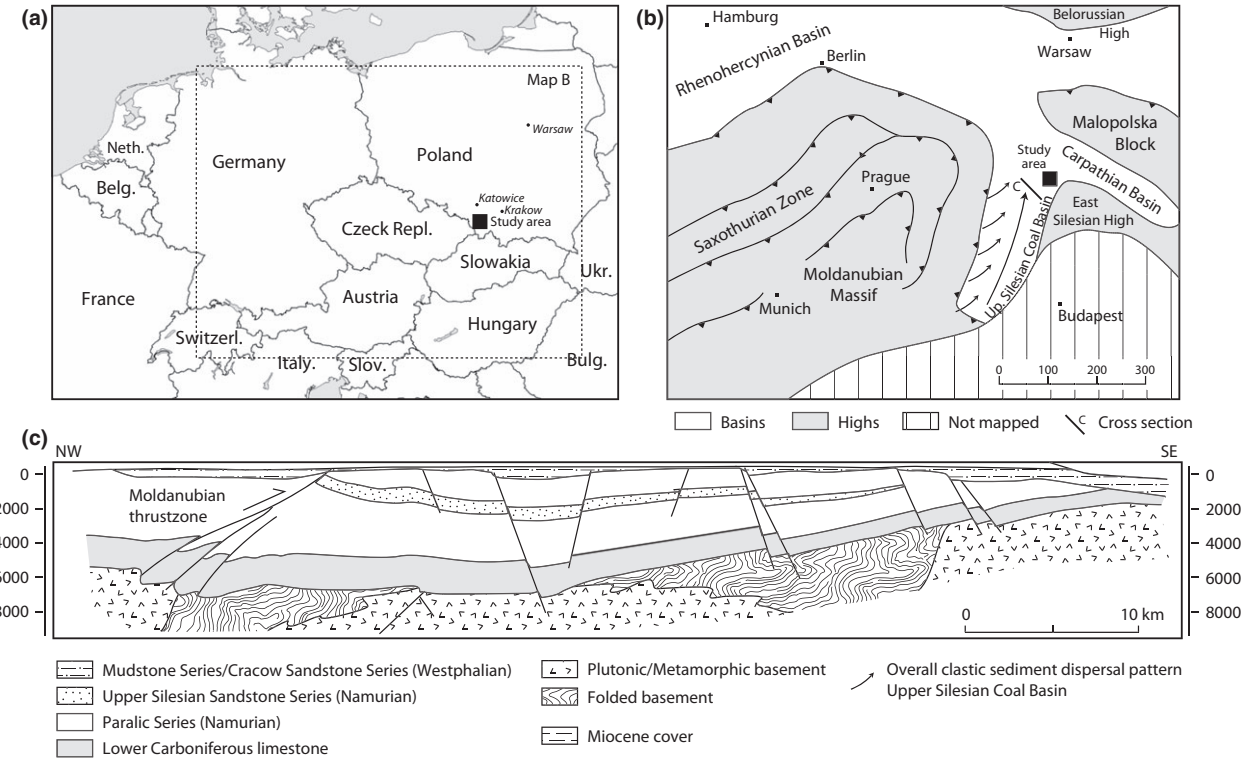

Fig. 2. Palaeogeographical and structural setting of the Upper Silesian Coal Basin and the study area. (A) Map of Central Europe showing location of the study area, (B) Structural organization of north-central Europe during the Namurian (after Ziegler, 1990), (C) NW-SE cross-section through the northern part of the Upper Silesian Coal Basin close to the study area (after Kotas, 1994).

of thick peat bodies. For instance, the thickness of coal bed 510, which constitutes the base of the USSS, increases from 6 m in the study area to 24 m in the east.

The overlying Mudstone Series is dominated by meandering channel and floodplain deposits (Doktor & Gradzinski, 1985; Gradzinski *et al.*, 1995). It is unconformably overlain by the Cracow Sandstone Series (Westphalian C-D), a unit dominated by sandy and conglomeratic braided-fluvial-channel deposits (Gradzinski *et al.*, 1995; Doktor, 2007) that displays overall north–north-eastward sediment transport as well (Kotas, 1995). In the east, the Cracow Sandstone Series is unconformably overlain by red and variegated sediments without any intercalated coal beds; these are probably of Stephanian age (Zdanowski & Zakowa, 1995). The Pennsylvanian section is truncated by an Alpine unconformity and is overlain by Miocene marls, with the depth of truncation increasing westwards (Fig. 2).

Study area

This study is based on sedimentary records of eight boreholes and fault maps from a 5 km^2 area within the 'Silesia' coal-mining concession. The area is located approximately 40 km south of the city of Katowice in southern Poland (Fig. 4). The youngest Pennsylvanian deposits in the area are Westphalian C sandstones of the Cracow Sandstone Series; these are buried below a *ca* 250 m Miocene cover (Van Bergen *et al.*, 2006). The stratigraphic interval under investigation comprises the USSS and the basal section of the conformably overlying Mudstone Series. In the study area, this interval is present at depths between 950 and 1250 m.

The concession area is dissected by two sets of steep faults that strike NE–SW and NW–SE (Fig. 4). The faults intersect at *ca* 60° angles and the NW–SE striking faults abutt the NE–SW striking faults. Offset of coal beds indicates normal displacement. Both the steepness of the faults and the 60° to 70° intersection angles of the two sets point to normal reactivation of an original strike-slip fault system, possibly related to Late Devonian dextral shear (Ziegler, 1990). The E–W trending fault that defines the southern margin of the coal-mining concession area is of Alpine origin (Van Bergen *et al.*, 2006).

The study area is located at the eastern end of the coal-mining concession area (Fig. 4). It is characterized by a major NE–SW trending normal fault (F1) that separates a footwall block in the south-west (fault block I) and a

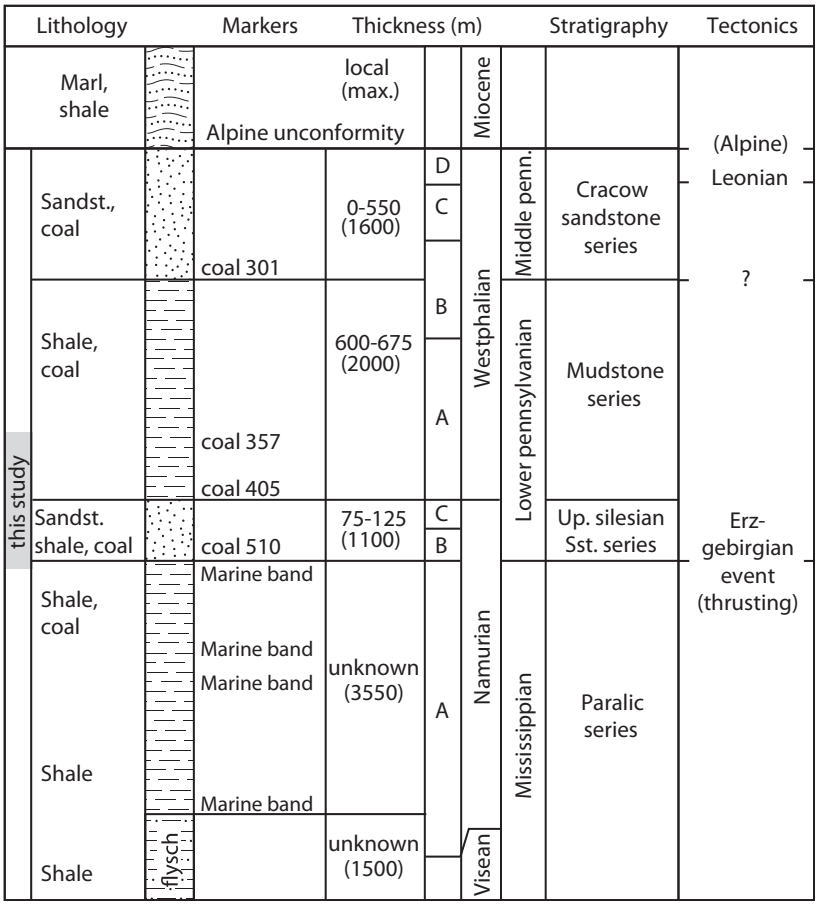

Fig. 3. Stratigraphic column for the Upper Silesian Coal Basin. Major coal beds/zones and marine bands are after Kotas (1994); thickness values are for the study area, maximum thickness in the basin are given between brackets.

composite hangingwall block in the north-west. This hangingwall block consists of two higher order fault blocks (II and III) that are separated by fault F2. Note that fault block II is part of the hangingwall block of fault block I, but it also serves as a (higher order) footwall block to fault block III. Extrapolation of coal-bed depth trends, observed on mining company cross-sections, has indicated the presence of a fault between well Si-18 and MB-90 (Fig. 4), the exact orientation of which is not known.

SEDIMENTARY FRAMEWORK

The sedimentary framework is based on core descriptions, wireline logs and coal-bed depth/thickness maps. The available core descriptions were drafted for coal-exploration purposes, with a lithology record but lacking descriptions of sedimentary structures. From regional work it is known that the USSS generally comprises alternating floodplain and coastal-plain mudstones, coal beds and braided fluvial sandstones; marginal marine shales are restricted to the interval below coal bed 405 (Kotas, 1994; Zdanowski & Zakowa, 1995). The elementary character of the sedimentary descriptions did not permit the recognition of, for example, lacustrine intercalations within floodplain shales, or the distinction between small fluvial-channel and thin crevasse delta deposits. Some of the interpretations may therefore be slightly simplified.

Figure 5 shows N-S and E-W correlation panels based on coal-bed interpretations of the mining company, using regional coal-bed terminology. The studied interval, comprising the USSS and the lower 50 m of the Westphalian Mudstone Series is characterized by four relatively thick, correlatable coal beds (510, 405, 401, 354). These main coal beds define three (major) sedimentary units (Unit 1 to 3) with an average thickness that decreases upwards from 115 m to 50 m. Units 1 and 2 have a distinct wedge shape and thicken to the north-west. Unit 3 has a more tabular shape. Internally, each unit is composed of three to four (preserved) sedimentary cycles, which are typical cyclic alternations of fluvial sandstone, grey floodplain or delta-plain mudstones and coal beds (cyclothems). Units 1 and 2 are dominated by thick, laterally extensive

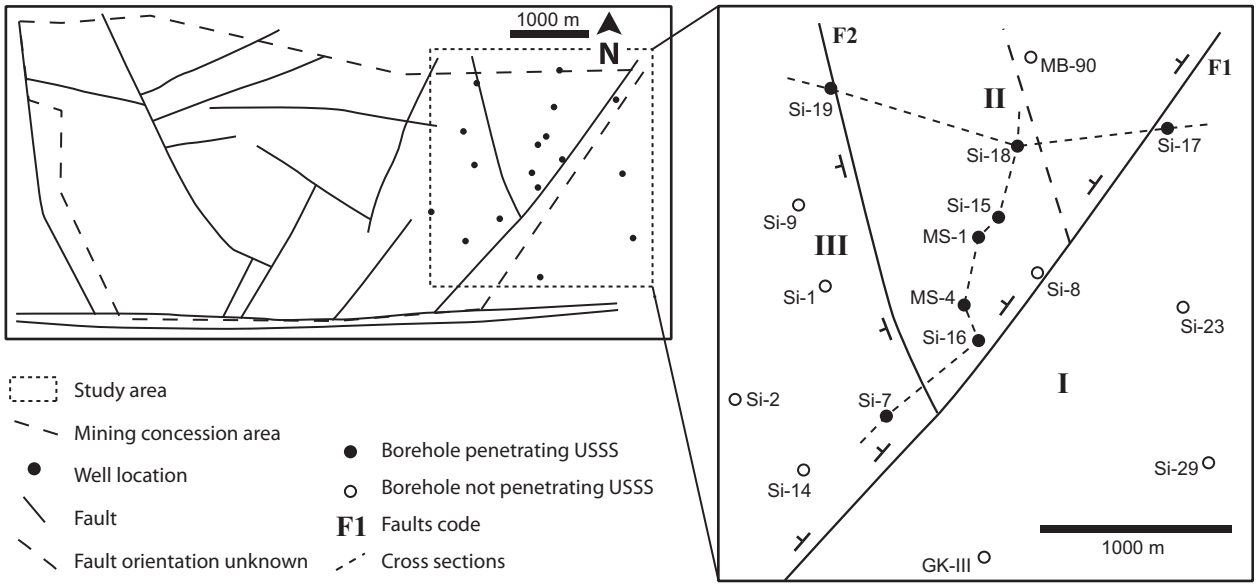

Fig. 4. Map of the Silesia mining concession showing major faults and borehole locations for the study area. The study area covers 3 fault blocks (numbered I to III) with densely spaced boreholes. Wells not incorporated in the cross-sections do not penetrate the studied interval or only partly and were therefore not included in the quantitative analysis (open circles).

sandstone bodies, whereas the sandstone bodies in Unit 3 are thinner and more isolated.

Thick sandstone bodies are numerous in Units 1 and 2; they alternate with laminated and rooted grey mudstone intervals and coal beds. Their number decreases upwards from Unit 1 (average sandstone content *ca* 55%) to Unit 2 (*ca* 30%). Thick sandstone bodies have not been encountered in Unit 3. The bodies are between 10 and 20 m thick and most of them appear laterally extensive. Occasionally, sandstone bodies in the vicinity of faults wedge out towards adjacent boreholes (e.g. borehole Silesia-18/19). Towards the downthrown sides of faults, thick sandstone bodies are more numerous and occur stacked into compound bodies, and their cumulative thickness gradually increases. This suggests that channels preferentially followed fault trajectories (Fig. 5, inset).

Thin, isolated sandstone bodies are observed in all three units. They are most pronounced in Unit 3, where they make up *ca* 10% of the succession. These sandstone bodies are usually only a few metres thick and cannot be traced to neighbouring boreholes. In contrast to the thick fluvial sandstones that dominate Units 1 and 2, these channel sands are encased in floodplain fines.

Coal beds are present throughout the sequence and occur in distinct bundles. Two types of coal bed characterize the study area. The first type comprises thick coal beds (1 to 6 m) that are present across the entire study area (Fig. 5). The other type comprises non-continuous thin coals (<1 m); these wedge out laterally or are possibly truncated by fluvial-sandstone bodies. Coal beds show pronounced thickness variation across the study area. For example, the thickness of coal bed 510 increases from 0·6 m (Silesia-17) to 6 m (Silesia-19) over a distance of *ca* 3 km.

Interpretation

The thick, laterally extensive sandstone bodies that dominate Units 1 and 2 have dimensions in the range of major fluvial-sandstone bodies in the Pennsylvanian of Europe and North America (Fielding, 1984a; Aitken & Flint, 1995; Jones & Glover, 2005; Greb *et al.*, 2008). In general, Pennsylvanian fluvial systems are interpreted as sheet-like fluvial-braidplain deposits with erosional basal surfaces (Haszeldine & Anderton, 1980; Jones & Hartley, 1993; Jones & Glover, 2005) or as incised valley deposits (Aitken & Flint, 1995; Hampson *et al.*, 1999). Based on their sheet character and the regular alternations with mudstone and coal, the majority of the major sandstones in the study area are interpreted as the deposits of laterally extensive fluvial-braidplain systems. Some of the sandstone bodies in the vicinity of faults, however, wedge out rapidly away from these fault, which could point to channels incising into the substrate where subsidence is highest. The thin, isolated sandstone bodies encased in floodplain mud are interpreted as the deposits of small channels meandering across the floodplain. Other types of floodplain sandstones, such as crevasse splays, may be represented as well

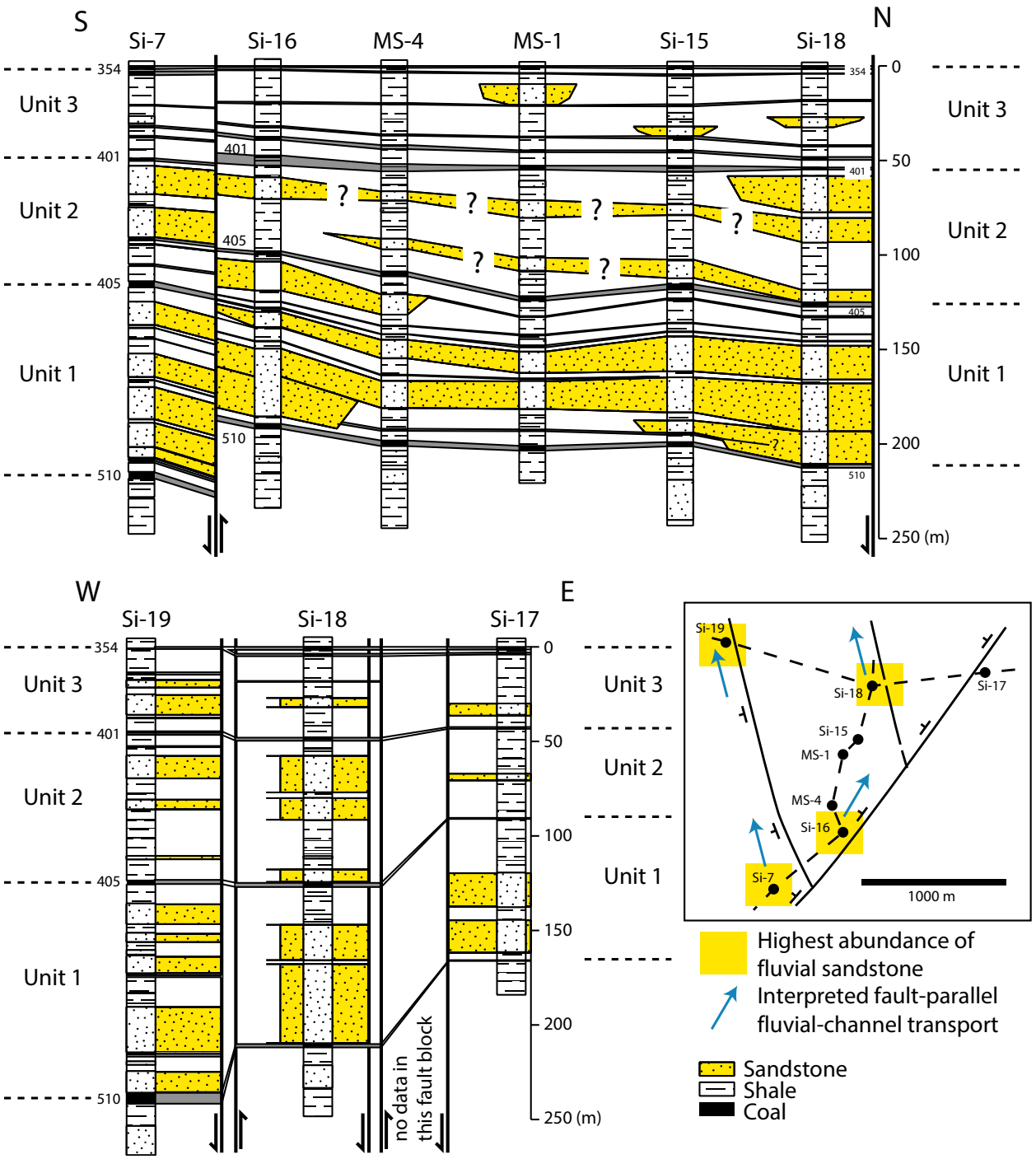

Fig. 5. Correlation panels showing north–south and east–west transects through the study area. Correlations based on coal-bed stratigraphy. Sandstone bodies seem well correlatable in the lower part of the studied interval; correlations in the middle part are more tentative. Numbers 510, 405, 401 and 354 indicate major coal beds.

(Fielding, 1986), but could not be confidently distinguished due to the rudimentary nature of the data set.

Thick upper Carboniferous coal beds are commonly interpreted as coastal-plain and floodplain peat accumulations (Fielding, 1984b; McCabe, 1984) and, based on the associated facies, the coals in the study area are probably floodplain coals. The great thickness and lateral extent of some of the coals indicate that peat swamps were exten-

Table 1. Thickness and lithological data for the studied interval (between coal beds 354 to 510).

Borehole	Sediment column (m)	Lithology (cumulative thickness)				Lithology				Deviation from mean				
		Sandstone (m)	Coal (m)	Mudstone (m)	Mudstone + coal (m)	Sandstone (%)	Coal (%)	Mudstone (%)	Mudstone + coal (%)	Sediment column (%)	Sandstone (m) (%)	Coal (m) (%)	Mudstone (m) (%)	Mudstone + coal (m) (%)
Silesia-07	218	94	1	107	124	43·1	7·8	49·1	56·9	6·2	13·9	37·8	−3·2	−3·9
Silesia-15	202	69	15	118	133	34·2	7·4	58·4	65·8	−1·6	−16·4	21·6	6·8	3·1
Silesia-16	192	70	11	111	122	36·5	5·7	57·8	63·5	−6·5	−15·2	−10·8	0·5	−5·5
Silesia-17	166	44·5	4·5	117	121·5	26·8	2·7	70·5	73·2	−19·2	−46·1	−63·5	5·9	−5·9
Silesia-18	213	104	12·5	96	108·5	48·9	5·9	45·2	51·1	3·5	26·1	1·4	−13·1	−15·9
Silesia-19	242	114	14	114	128	47·0	5·8	47·2	53·0	17·6	37·6	13·5	3·2	−0·8
MS-1	204	62·5	13·5	128	141·5	30·6	6·6	62·7	69·4	−0·6	−24·2	9·5	15·8	9·6
MS-4	201	47	10·5	143·5	154	23·4	5·2	71·4	76·6	−2·1	−43·0	−14·9	29·9	19·3
Mean	205	83	12	111	129	39	6	55	55					
Correlation coefficient (with sediment column thickness)		0·84	0·78	−0·20	0·00									

sive and built considerable peat accumulations over prolonged periods. The thin, non-continuous coal beds probably formed in local depressions, such as lakes and abandoned channels (cf. Greb & Chesnut, 1992). The change in coal thickness over short distances may be related to infilling of inherited floodplain topography (Greb & Chesnut, 1992; Greb *et al.*, 1999), but overall coal thickness increases towards the downthrown sides of faults, which indicates that synsedimentary faulting and related differential subsidence played a role (cf. Guion & Fielding, 1988; Greb *et al.*, 2002, 2005).

INFLUENCE OF FAULT-BLOCK ROTATION ON SEDIMENTATION

Regional subsidence variations were approximated by measuring the thickness of the studied interval (coal-bed interval 354 to 510) and the thickness of the three units at the borehole locations (Table 1). This approach provides a reasonable approximation because the occurrence of coal beds throughout the sequence indicates deposition near base level (Bohacs & Suter, 1997), i.e. at or close to sea-level, and also that sedimentation overall kept up with subsidence. The studied interval contains relatively equal amounts of mudstone at the various borehole locations (Table 1), so that the thickness variations cannot be due to differential compaction of mud. Because coal is more abundant in the thicker sequences, the thickness variations of the studied interval cannot be attributed to preferential compaction of peat. Also note that Nadon (1998) has shown that the deep burial compaction of peat, long considered to be around 10 : 1 (McCabe, 1984), is not higher than *ca* 2·5 : 1 which equals the compaction of mud. This ratio applies because most compaction occurs in the plant-to-peat rather than the peat-to-coal stage (Van Asselen *et al.*, 2010).

Thickness maps

In Fig. 6 thickness maps are shown for the studied interval and for the individual Units 1 to 3. Map *a* shows the variation in thickness of the entire sediment column (between coals 510 to 354); it ranges from 166 m (Silesia-17) on fault block I to 242 m on fault block III (Silesia-19). With a mean thickness of 205 m these extremes reflect a differential-subsidence range between −19% and +18% (Table 1). The data further show that the thickness increases northwards across fault blocks II and III.

Figure 6B shows the variation in interval thickness for Unit 1. The unit has a maximum thickness of 119 m in borehole Silesia-19 and minimum thickness of 76 m in borehole Silesia-17. With an average thickness of 94 m, differential subsidence ranges between −18% and +28%.

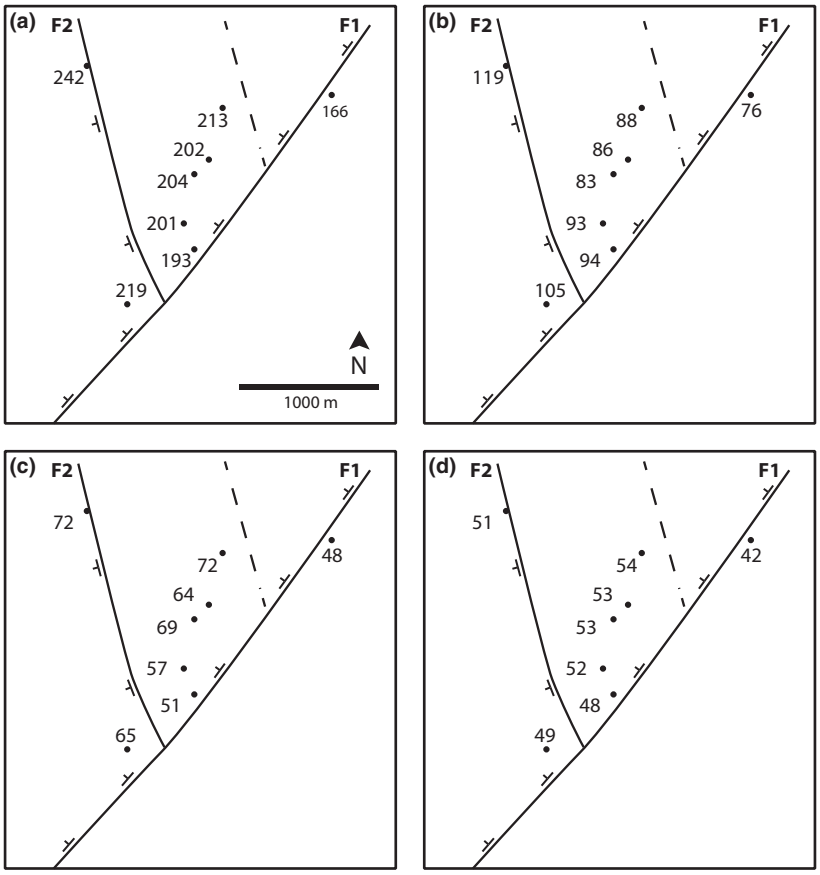

Fig. 6. Thickness maps for the studied stratigraphic interval. (A) complete interval, (B) Unit 1, (C) Unit 2 and (D) Unit 3.

The thickness of Unit 1 on fault block II shows a slight southward increase from 88 to 94 m; on block II the unit thickness increases from 105 to 119 m northward.

In Fig. 6C the thickness variation for Unit 2 is shown. In borehole Silesia-19, the unit has a maximum thickness of 72 m; it has a minimum thickness of 48 m in borehole Silesia-17. The mean thickness is 62 m, giving a differential-subsidence range from −23% to +16%. On fault block II the thickness increases northwards from 51 to 72 m and on fault block III the thickness increases northwards as well, from 65 to 79 m.

Figure 6D shows the thickness variation for Unit 3. It is characterized by a fairly constant thickness of 48 m to 54 m across most of the study area, indicating little differential subsidence, ranging between −5% and +8%. Borehole Si-17 on fault block I shows a more reduced thickness of 42 m (−17%).

Subsidence history

The maps of Fig. 6 indicate that the thickness variations are not random, but follow directional trends. The data indicate that much of the difference in thickness can be attributed to relative movements between fault blocks, but thickness changes on individual fault blocks indicate that rotation of fault blocks contributed considerably.

Subsidence rates were lowest in the south-east and increased overall to the north-west. A reduced thickness for all units in borehole Silesia-17 indicates that fault block I served as a footwall block to fault blocks II and III. Fault block III experienced the highest subsidence rates; during the deposition of Units 1 and 2 it subsided more rapidly than the fault blocks to the east and south-east. The rather constant thickness of Unit 3 north of fault F1 indicates that differential subsidence between fault blocks II and III came to a halt after deposition of Unit 2, and that they continued to subside as a compound block, only slightly faster than fault block I.

The thickness differences indicate that differential subsidence was greatest during and shortly after deposition of coal bed 510 and had mostly ceased after deposition of Unit 2, the top of which marks the Namurian-Westphalian boundary. This boundary coincides with the end-

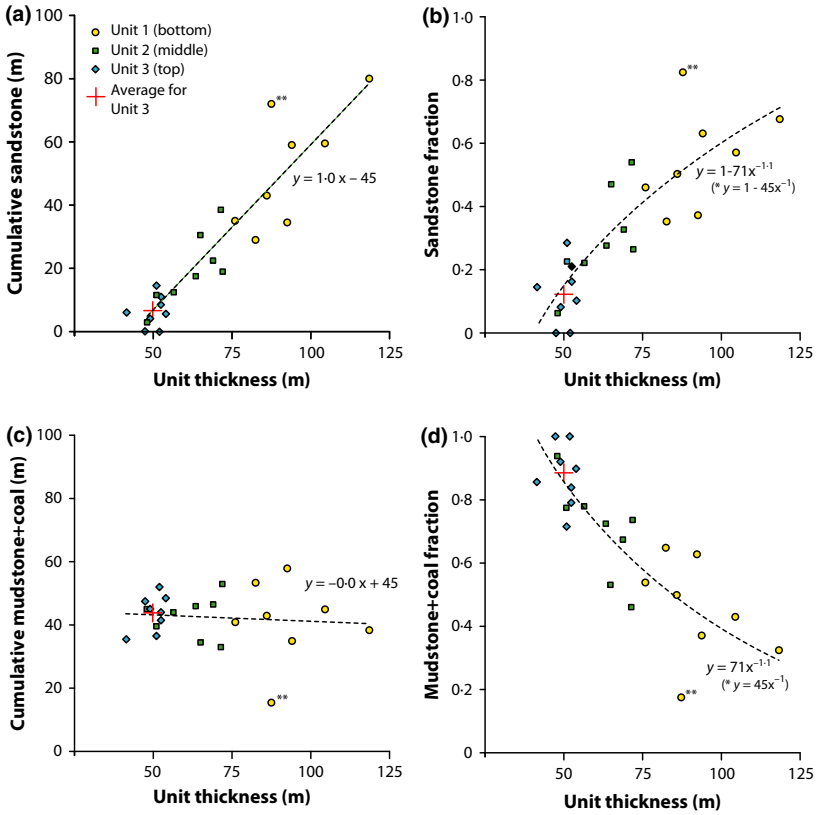

Fig. 7. Cross-plots of lithological thickness data versus cycle thickness. (A) cumulative-sandstone thickness, (B) sandstone fraction, (C) cumulative-mudstone/coal thickness and (D) mudstone/coal fraction. *Regression equation with outlier** excluded.

Namurian termination of the 'Erzgebirgian' thrusting event (Kotas, 1994), possibly indicating that thrusting events caused immediate loading-induced subsidence, which was accommodated by normal displacement of the block-faulted basement. Then, when thrusting came to a halt subsidence was dominated again by background subsidence.

Thickness variations on individual fault blocks point to superimposed rotation, which was consistently northwards for fault block III, whereas fault block II rotated northwards during the deposition of Unit 2 and shows a westward or south-westward rotational component during the deposition of Unit 1. For the other fault blocks, the rotation history could not be reconstructed due to limited borehole control.

Fluvial transport directions

Due to data limitations, there is no detailed information on sandstone-body orientation or palaeocurrent directions, other than regional information indicating overall north to north-eastward fluvial transport. However, the distribution of sandstone bodies may give some general information about their orientation. The correlation panels (Fig. 5) show that fluvial-sandstone bodies are more numerous and have a greater combined thickness at the downthrown sides of faults, i.e. in wells Si-7, Si-16, Si-18 and Si-19. This is taken as an indication that the channels flowed primarily parallel to these faults, as indicated on the inset of Fig. 5.

Note that the orientation of faults in the study area is such that the overall transport direction of the fluvial systems is consistent with the large-scale, north–north-westward direction observed for the basin during deposition of the USSS (Kotas, 1994; Zdanowski & Zakowa, 1995).

QUANTITATIVE ANALYSIS OF SEDIMENT DISTRIBUTION

To assess the mechanism that controlled sediment distribution, a quantitative analysis of the influence of subsidence on the distribution of sandstone, mudstone and coal was carried out for the entire studied interval (between coal beds 510 and 354) and for the three units separately.

Cumulative thicknesses and proportions of the different lithologies are presented in Table 1. A positive correlation of 0·84 exists between the thickness of the studied interval

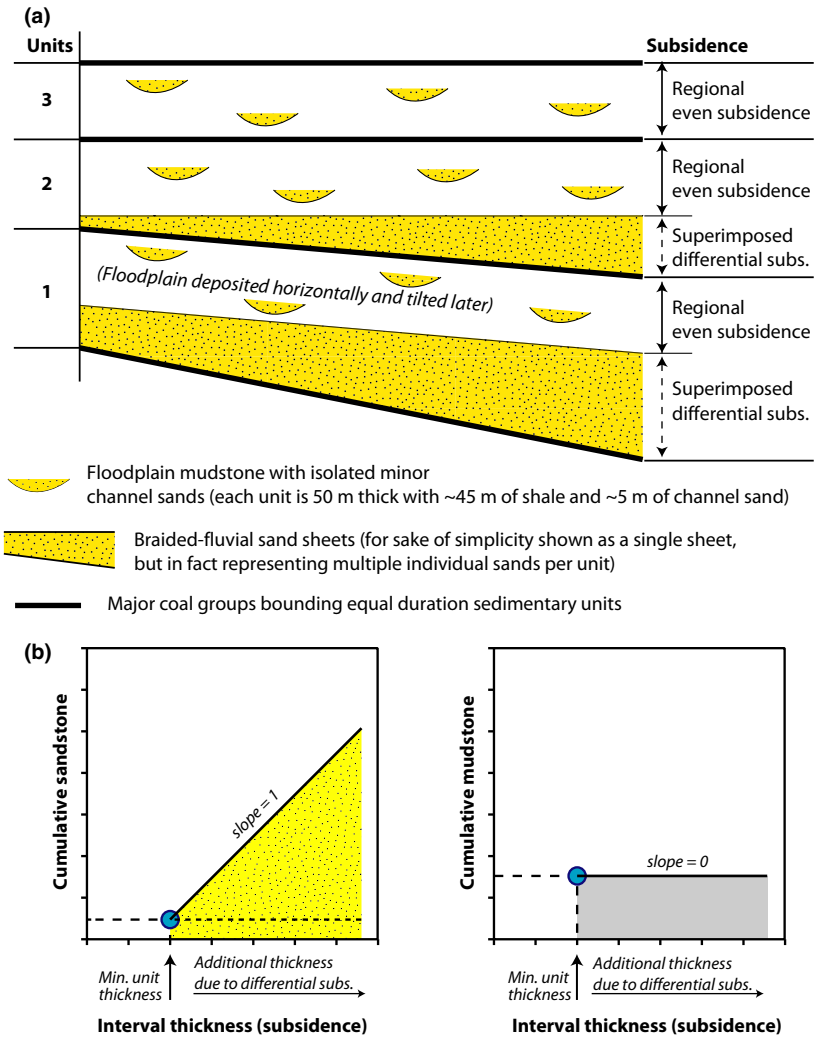

Fig. 8. Diagram showing (A) the overall distribution of braided-fluvial sands and coal-bearing floodplain deposits in Units 1, 2 and 3; and (B) cross-plot trends for cumulative-sandstone and cumulative-mudstone thickness.

and the cumulative-sandstone thickness (Table 1, Fig. 7A). This correlation is to be expected, because an overall thicker sequence is likely to contain more sandstone than a thin sequence, but the percentage of sandstone increases with increasing interval thickness as well. A similar relationship is observed for coal, with higher values for cumulative coal thickness and coal percentage where the thickness of the studied interval is greater (correlation coefficient: 0·78). Conversely, the cumulative-mudstone content shows a slightly negative correlation (−0·20) with interval thickness. Note, however, that the cumulative thickness of mudstone and coal (those lithologies added) shows a correlation coefficient of zero with interval thickness.

The cross-plots in Fig. 7 show that the strong positive correlation between interval thickness and cumulative-sandstone thickness is maintained at the scale of individual units. Note that the cumulative-sandstone-thickness data for each unit constitute a well-defined data cluster in the cross-plot, and that only the data for Units 1 and 2 overlap slightly. The plots for the cumulative mudstone/coal thickness and the mudstone/coal percentage (Fig. 7C) show that the three units contain approximately equal amounts of mudstone/coal (*ca* 45 m), and that no relationship exists between unit thickness and mudstone/coal content. Figure 7A further shows that a single regression line fits the sandstone values for all three units, and that this line originates from the mean of the data cluster for Unit 3, which is the unit that hardly experienced superimposed differential subsidence. This mean value represents a thickness of 50 m, comprising *ca* 45 m of mudstone/coal and *ca* 5 m of minor-channel sandstone on average. The fact that the regression line originates from this mean value indicates that each other unit is

essentially a Unit-3 unit complemented by a differential-subsidence dependent amount of sandstone. The regression-line equation for mudstone/coal ($y = 0{\cdot}0x + 45$) reflects that the amount of mudstone/coal equals *ca* 45 m at all borehole locations and its slope of 0 stresses the independence of differential subsidence. The regression-line equation for sandstone ($y = 1{\cdot}0x - 45$) with a slope of 1 shows that all accommodation space, minus the 45 m for mudstone and coal, comprises sandstone.

In Fig. 8, the above interpretation is shown diagrammatically. The fact that amounts of mudstone and coal in each cycle are regionally constant indicates that all mudstone and coal was deposited when the depositional plain experienced laterally even subsidence. If mudstone and coal would have been deposited during phases of differential subsidence as well, then some additional floodplain mudstone/coal deposition would be expected in areas of higher subsidence, as predicted by the LAB-models (see Fig. 1; Bridge & Mackey, 1993). That each cycle contains the same cumulative thickness of mudstone and coal (*ca* 45 m) further suggest that the three coal group-bounded units represent equal time periods, during which long-term subsidence resulted in regionally constant, relatively slow creation of accommodation space. That thick coal-bounded units represent equal time periods is a common interpretation for Pennsylvanian sequences, attributed to strong glacio-eustatic control (Klein & Willard, 1989; Greb *et al.*, 2008), and such cycles are typically thought to be short eccentricity (100 kyr) or long-eccentricity (400 kyr) cycles (Heckel, 1986, 2008).

That the cumulative-sandstone thickness is much higher in areas of stronger subsidence while equal amounts of mudstone/coal are present at each borehole location indicates that fault-block tilting was episodic, only shortly interrupting background subsidence. When differential subsidence commenced, it resulted immediately in an overall change from accumulation of floodplain mud and associated minor-channel sands to bypassing of mud and accommodation of sand-sized sediment only.

SYNTECTONIC DEPOSITIONAL MODEL

As explained above, the alternation of tabular mudstone/coal deposits, with encased small-scale fluvial-channel sandstone, and wedge-shaped fluvial-braidplain deposits reflects that continuous, regionally constant subsidence was at times overprinted by pulses of fault-block rotation. It is envisaged that thrusting-induced loading was accommodated by reactivation of the block-faulted basement.

In Fig. 9, a depositional model is depicted that shows how periodic fault-block tilting superimposed on regional subsidence, explains the sediment distribution. An overall level depositional plain, characterized by depositional topography only, existed when regionally constant subsidence prevailed. The absence of a strong depositional gradient permitted standing water, thus promoting the settling of fine-grained sediment and the accumulation of

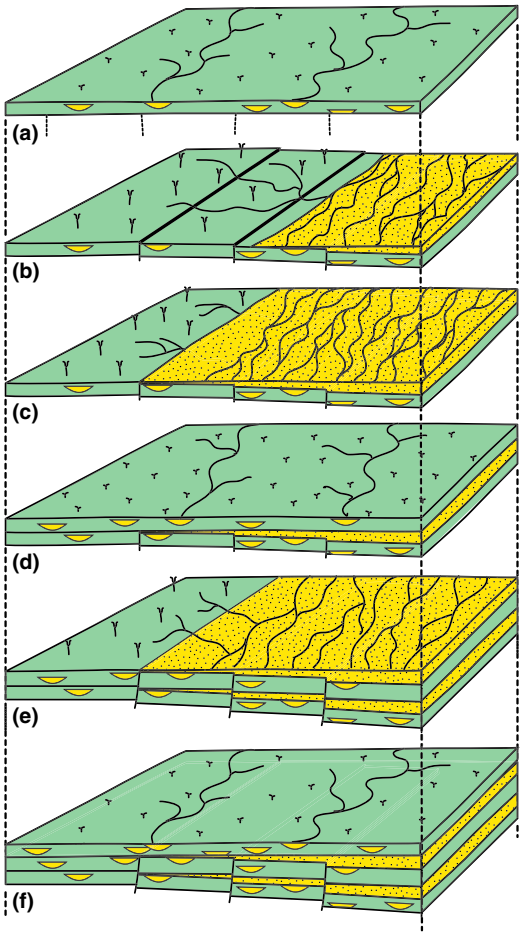

Fig. 9. Depositional model for fluvial deposition on top of faulted topography where tilting has a downstream component. (A) Under conditions of regionally constant subsidence a level floodplain should exist. Floodplain deposition is dominated by overbank mudstone, with small channels, contained within stable vegetated levees, distributed randomly. Dashed vertical lines below the floodplain indicate hidden, temporarily inactive faults; (B) When faulting occurs, additional accommodation space is created which becomes occupied by a high-energy braidplain system, eventually filling up the faulted topography (C); note that laterally the floodplain is a surface of non-deposition. The existence of a gradient in the downstream direction results in bypassing of the mud fraction, and allowing deposition of sand only. (D) Once faults become inactive and the available accommodation space has been filled by the braidplain system, a level depositional plain is re-established, and floodplain deposition takes over again. (E & F) Alternating periods of floodplain deposition and braidplain deposition result in a stacking of (i) tabular units consisting of mudstone, coal and rare isolated sandstone bodies and (ii) wedge-shaped sandstone bodies.

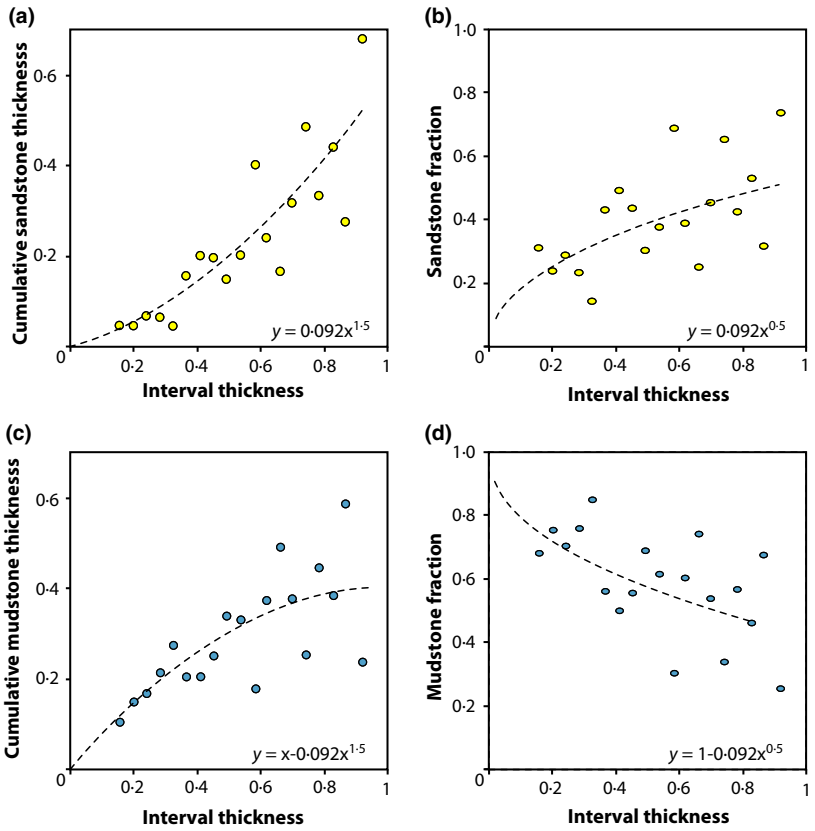

Fig. 10. Cross-plots determined for the LAB-model sequence in Figure 1.

peat (Fig. 9A). Channels flowed across the floodplain and experienced regular avulsions, resulting in a more or less random sandstone distribution. This random distribution is considered the direct result of constant subsidence rates throughout the area, i.e. there were no low-lying areas that preferentially attracted channel systems (cf. Alexander & Leeder, 1987).

Thrusting events caused periodic rotation of basement fault blocks and tilting of the depositional plain in various directions, but mostly with a northward-tilting component, i.e. in the direction of regional downbasin fluvial transport, which led to the interruption of floodplain conditions. It is thought that tilting was too fast for the fluvial system to compensate by means of aggradation and thus developed a depositional gradient (cf. Heller & Paola, 1996; Connell *et al.*, 2012). This gradient then resulted in bypass of fines downbasin. Fluvial sand accumulated in the low-lying areas, probably in braidplain systems, adapting and building to the new base-level profile (Fig. 9B). The braidplain systems quickly filled the newly available accommodation space (Fig. 9C). Once the fault activity had stopped, and the faulted topography had been levelled, a horizontal floodplain depositional system was re-established (Fig. 9D).

Coal beds are slightly thicker in areas of higher subsidence, although they are part of the tabular floodplain layers. This may be because peat swamps were formed where the groundwater level was highest during the transition from braidplain to floodplain, i.e. when the area was not completely level. Such a floodplain arrangement, with swamps preferentially on the hangingwall blocks, may have been maintained during the subsequent floodplain phase; also because peat lands may have grown well above the ground-water table.

Repeated alternations of floodplain and braidplain conditions resulted in the architecture depicted in Fig. 9E, with wedge-shape sandstone layers alternating with more tabular, mudstone-dominated layers. The thickness of these layers is variable, depending on the frequency and intensity of thrusting and fault-block rotation events. Note that the model presented here applies to low base-level situations only, otherwise faulting events would have resulted in the formation of lake bodies on top of the faulted topography (cf. Blair & Bilodeau, 1988).

Because the Pennsylvanian period was characterized by high-frequency sea-level fluctuations (Heckel, 1986; Rygel *et al.*, 2008), it is possible that infilling of the topography took place during transgressions, along the lines as

described for Pennsylvanian major fluvial-channel systems in other basins (Davies *et al.*, 1992; Aitken & Flint, 1995; Hampson *et al.*, 1999). The formation of those bodies is commonly explained in terms of aggradational infill of lowstand valleys in response to transgressions (Davies *et al.*, 1992; Shanley & McCabe, 1993).

The final situation (Fig. 9F) shows how two wedge-shape fluvial sandstone units are sandwiched between three tabular units of floodplain mudstone and randomly distributed minor-channel sands.

Lateral extent of fluvial-sandstone bodies

Within the study area there is no evidence of uplift of fault blocks during rotation, as the wedge-shaped units are thicker than the 50 m of the baseline unit at all locations. The major sandstone bodies are extensive and mostly run from fault to fault, their thickness gradually increasing towards areas of higher subsidence. Their regular, predictable distribution implies that the sandstone bodies are largely aggradational in nature and are hardly incised into the substrate, although minor erosion is bound to be associated with their basal scour surfaces.

The model predicts that the major sandstone bodies are continuous throughout the study area. Local deviations may result from, for example, the random distribution of small channels, the presence of mud-filled channels or differential compaction, but in a few boreholes the sandstone content deviates strongly. For instance, borehole Silesia-16 contains thick sandstone bodies at the base of Unit 1 that wedge-out over a few 100s of metres (Fig. 5). This borehole is located very close to a fault, where the subsidence rate was maximal. Such locations must have attracted most of the run-off and may have been more sensitive to erosion, resulting in local incision, either as isolated bodies or as localized deeper basal incisions at the base of aggradational sandstone sheets (Fig. 8).

Cyclothems and time

The above analysis indicates that the accumulation of the major sandstones occurred after faulting events. Hence, the apparent 'cyclothemic' alternation of fluvial sandstone, floodplain mudstone and coal beds, observed within the individual depositional units, is primarily of tectonic origin, rather than being controlled by glacio-eustasy. This conclusion is consistent with interpretations by others for sandstone-rich Pennsylvanian successions, that cyclothemic arrangement has a strong tectonic overprint or is tectonically controlled (Klein & Willard, 1989; Klein & Kupperman, 1992; Jones & Glover, 2005; Greb *et al.*, 2008). As discussed in more detail above, however, the actual infilling of the accommodation space generated by tilting may have taken place during transgressions.

The three coal-bounded units that constitute the main sedimentary framework were likely eustatically controlled, because the equal amounts of mudstone/coal in the units, deposited under conditions of regionally constant subsidence, point to an equal duration. On a large scale, cyclothem sequences are generally believed to be built of sedimentary cycles representing short and long eccentricity (Greb *et al.*, 2008; Heckel, 2008). Based on a minimum thickness of 50 m for each of the three units, and considering the fact that the study area is located at the low-subsidence, eastern end of the basin, long eccentricity is the more likely candidate. It requires a net, post-compaction subsidence rate of *ca* 12 cm kyr^{-1}, compared to more than 50 cm kyr^{-1} for short eccentricity. Based on local and maximum Westphalian A-B stratigraphic thickness values (650 to 2000 m; Fig. 2), and a duration for that interval of about 3 to 4 Ma (Gradstein *et al.*, 2004), subsidence must have been in the range of max. *ca* 65 cm kyr^{-1} near the thrust belt to min. *ca* 15 cm kyr^{-1} in the study area, which further supports the long-eccentricity interpretation.

DISCUSSION AND CONCLUSIONS

This study demonstrates that differential subsidence had a strong control over the lateral and vertical distribution of sandstone, mudstone and coal. Sandstone content increases more than linearly towards the areas of higher subsidence. This outcome is close to LAB-model predictions (Allen, 1978; Bridge & Leeder, 1979; Bridge & Mackey, 1993; Mackey & Bridge, 1995), but the lateral distribution of mudstone is intrinsically different. The work by Alexander & Leeder (1987), Leeder & Gawthorpe (1987) and subsequent LAB-model results predict that, despite a decrease in mudstone percentage, the cumulative floodplain-mudstone thickness increases towards the downthrown side of a fault. In the study area, the amount of floodplain mudstone is constant, hence independent of subsidence.

A number of geological circumstances may explain why the observed alluvial architecture does not fully comply with the standard model. Faulting and associated differential subsidence were intense and probably episodic, thus causing relatively steep gradients, also in the downbasin direction. This condition may have prevented the fluvial systems from maintaining a level floodplain by means of aggradation (Heller & Paola, 1996; Kim *et al.*, 2010; Connell *et al.*, 2012) and causing bypass of fine-grained sediment further downstream. In addition, the studied sediments are from a time period when glacio-eustatic sea-level fluctuations were prominent. It is possible that lowstands of sea-level, concurrent with faulting episodes,

further enhanced gradients, and during subsequent transgression promoted infilling of tectonic accommodation space with the sandy sediments of braided-fluvial systems, in the same way that lowstand valleys are filled by aggrading fluvial systems under conditions of rising sea-level (Shanley & McCabe, 1993).

For the sake of comparison, a quantitative analysis was performed on the LAB-model half-graben cross-section of Bridge & Mackey (1993, shown here as Fig. 1), the results of which are shown in Fig. 10. There is quite a bit of data scatter, because of the low number of channels in the sediment volume in combination with their random distribution. However, the cross-plots clearly show that the increase of cumulative-sandstone with increasing interval thickness (subsidence) is not linear, but probably follow a power law ($y = ax^b$), i.e. the sandstone thickness increases more than linearly with subsidence. At the same time cumulative-mudstone increases less than linearly with subsidence ($y = x - ax^b$). At first glance, the data clouds may actually suggest a linear relationship, but it should be taken into account that a linear trend line must intersect the origin of the graph (0,0), because the standard model is based on rotational subsidence only (Fig. 1). Hence, where subsidence is zero, or approaches it, cumulative-sandstone and cumulative-mudstone thickness must be zero as well. The studied sequence, by comparison, experienced rotational subsidence superimposed on regional background subsidence, which resulted in the creation of accommodation space across the entire area (at least 50 m per unit). Therefore, the linear trend line does not intersect the origin of the graph, but originates from the point for which $x = 50$ and $y = 5$ (Fig. 7A). This point represents the minimal unit thickness of 50 m and the average cumulative-sandstone thickness of *ca* 5 m for such a unit.

Both mechanisms result in a high sandstone fraction in areas of high subsidence, but sandstone-body width and interconnectedness are likely to be different. The LAB-models predict numerous sandstone bodies of limited lateral extent, which are likely to be vertically connected. The model described here predicts laterally extensive sandstone bodies that in most cases are vertically disconnected by intervening floodplain mudstones. In addition to the above-described local variations in sandstone percentage, such architectural differences should be taken into account when these models are used as a predictive tool in hydrocarbon exploration and production studies.

The study area is small, but the straightforward relationship with differential subsidence suggests that the mechanism at work is more widely applicable. This approach requires further quantitative testing, on other Pennsylvanian cyclothem sequences and on fluvial sequences from geological periods when high-amplitude sea-level fluctuations did not interfere.

ACKNOWLEDGEMENTS

This study originates from the RECOPOL field experiment for underground storage of carbon dioxide in coal beds in southern Poland, a project funded by the 5th framework of the European Commission. We are grateful to Chris Paola, an anonymous reviewer and journal editor Paul Carling for constructive comments and suggestions. Discussions with K. Geel, H. Pagnier and E. van der Most helped shape our ideas. The Central Mining Institute of Poland is thanked for providing access to the data.

References

Aitken, J.F. and **Flint, S.S.** (1995) The application of high-resolution sequence stratigraphy to fluvial systems: a case study from the Upper Carboniferous Breathitt Group, eastern Kentucky, USA. *Sedimentology*, **42**, 3–30.

Alexander, J. and **Leeder, M.R.** (1987) Active tectonic control of alluvial architecture. In: *Recent Developments in Fluvial Sedimentology* (Eds F.G. Ethridge, R.M. Flores and M.D. Harvey), *SEPM Spec. Publ.*, **39**, 243–252.

Allen, J.R.L. (1978) Studies in fluvial sedimentation: an exploratory quantitative model for the architecture of avulsion-controlled alluvial suites. *Sed. Geol.*, **21**, 129–147.

Allen, J.L. (1993) Lithofacies relations and controls on deposition of fluvial-deltaic rocks of the Upper Pocahontas Formation in southern West Virginia. *Southeast. Geol.*, **33**, 131–147.

Blair, T.C. and **Bilodeau, W.L.** (1988) Development of tectonic cyclothems in rift, pull-apart, and foreland basins: sedimentary response to episodic tectonism. *Geology*, **16**, 517–520.

Bohacs, K.M. and **Suter, J.** (1997) Sequence stratigraphic distribution of coaly rocks; fundamental controls and paralic examples. *AAPG Bull.*, **81**, 1612–1639.

Bridge, J.S. and **Leeder, M.R.** (1979) A simulation model of alluvial stratigraphy. *Sedimentology*, **26**, 617–644.

Bridge, J.S. and **Mackey, S.D.** (1993) A revised alluvial stratigraphy model. In: *Alluvial Sedimentation* (Eds M. Marzo and C. Puigdefabregas), *IAS Spec. Publ.*, **17**, 319–336.

Bryant, M., **Falk, P.** and **Paola, C.** (1995) Experimental study of avulsion frequency and rate of deposition. *Geology*, **23**, 365–368.

Collinson, J.D., **Jones, C.M.**, **Blackbourn, G.A.**, **Besly, B.M.**, **Archard, G.M.** and **McMahon, A.H.** (1993) Carboniferous depositional systems of the Southern North Sea. In: *Petroleum Geology of Northwest Europe: Proceedings of the 4th Conference* (Ed. J.R. Parker), *Geol. Soc. London*, **4**, 677–687.

Connell, S.D., **Wonsuck, K.**, **Paola, C.** and **Smith, G.A.** (2012) Fluvial morphology and sediment-flux steering of axial–transverse boundaries in an experimental basin. *J. Sed. Res.*, **82**, 310–325.

Davies, S.J. (2008) The record of carboniferous sea-level change in low-latitude sedimentary successions from Britain and Ireland during the onset of the late paleozoic ice age. In: *Resolving the Late Paleozoic Ice Age in Time and Space* (Eds C.R. Fielding, T.D. Frank and J.L. Isbell), *GSA Spec. Pap.*, **441**, 187–204.

Davies, H., **Burn, M.**, **Budding, M.** and **Williams, H.** (1992) High-resolution sequence stratigraphic analysis of fluvio-deltaic cyclothems: the Pennsylvanian Breathitt Group, east Kentucky. AAPG 1992 Annual Convention Programme, pp.27, *AAPG Search and Discovery Article #91012*.

Doktor, M. (2007) Conditions of accumulation and sedimentary architecture of the Upper Westphalian Cracow Sandstone Series (Upper Silesia Coal Basin, Poland). *Ann. Soc. Geol. Pol.*, **77**, 219–268.

Doktor, M. and **Gradzinski, R.** (1985) Alluvial depositional environment of coal-bearing "mudstone series" (Upper Carboniferous, Upper Silesian Coal Basin). *Stud. Geol. Pol.*, **82**, 5–67.

Ferm, J.C. and **Weisenfluh, G.A.** (1989) Evolution of some depositional models in Late Carboniferous rocks of the Appalachian coal fields. *Int. J. Coal Geol.*, **12**, 259–292.

Fielding, C.R. (1984a) Upper delta plain lacustrine and fluviolacustrine facies from the Westphalian of the Durham coalfield, NE England. *Sedimentology*, **31**, 547–567.

Fielding, C.R. (1984b) A coal depositional model for the Durham Coal Measures of NE England. *J. Geol. Soc. London*, **141**, 919–931.

Fielding, C.R. (1986) Fluvial channel and overbank deposits from the Westphalian of the Durham coalfield, NE England. *Sedimentology*, **33**, 119–140.

Fielding, C.R. and **Johnson, G.A.L.** (1987) Sedimentary structures associated with extensional fault movement from the Westphalian of NE England. In: *Continental Extensional Tectonics* (Eds M.P. Coward, J.F. Dewey and P.L. Hancock), *Geol. Soc. London. Spec. Publ.*, **28**, 511–516.

Gradstein, F.M., **Ogg, J.G.** and **Smith, A.G.** (2004) *A Geologic Time Scale 2004*. Cambridge University Press, Cambridge, 610 pp.

Gradzinski, R., **Doktor, M.** and **Slomka, T.** (1995) Depositional environments of the coal-bearing Cracow Sandstone Series (Upper Westphalian), Upper Silesia, Poland. *Stud. Geol. Pol.*, **108**, 149–170.

Greb, S.F. and **Chesnut, D.R.** (1992) Transgressive channel filling in the Breathitt Formation (Upper Carboniferous), eastern Kentucky coal field, USA. *Sed. Geol.*, **75**, 209–221.

Greb, S.F., **Eble, C.F.** and **Hower, J.C.** (1999) Depositional history of the Fire Clay coal bed (Late Duckmantian), Eastern Kentucky, USA. *Int. J. Coal Geol.*, **40**, 255–280.

Greb, S.F., **Eble, C.F.**, **Hower, J.C.** and **Andrews, W.M.** (2002) Multiple-bench architecture and interpretations of original mire phases—Examples from the Middle Pennsylvanian of the Central Appalachian Basin, USA. *Int. J. Coal Geol.*, **49**, 147–175.

Greb, S.F., **Eble, C.F.** and **Hower, J.C.** (2005) Subtle structural influences on coal thickness and distribution: examples from the Lower Broas-Stockton coal (Middle Pennsylvanian), Eastern Kentucky Coal Field, USA. In: *Coal Systems Analysis* (Ed. P.D. Warwick), *Geol. Soc. Am. Spec. Pap.*, **387**, 31–50.

Greb, S.F., **Pashin, J.C.**, **Martino, R.L.** and **Eble, C.F.** (2008) Appalachian sedimentary cycles during the Pennsylvanian: changing influences of sea level, climate, and tectonics. *Geol. Soc. Am. Spec. Pap.*, **441**, 235–248.

Guion, P.D. and **Fielding, C.R.** (1988) Westphalian A and B Sedimentation in the Pennine Basin, UK. In: *Sedimentation in a Syn-orogenic Basin Compex: The Upper Carboniferous of Northwest Europe* (Eds B.M. Besly and G. Kelling), pp. 153–177. Blackie, Glasgow.

Guion, P.D. and **Rippon, J.H.** (1995) The Silkstone Rock (Westphalian A) from the east Pennines, England: implications for sand body genesis. *J. Geol. Soc. London*, **152**, 819–832.

Guion, P.D., **Fulton, I.M.** and **Jones, N.S.** (1995) Sedimentary facies of the coal-bearing Westphalian A and B north of the Wales-Brabant High. *Geol. Soc. London. Spec. Publ.*, **82**, 45–78.

Hajek, E.A., **Heller, P.L.** and **Sheets, B.A.** (2010) Significance of channel-belt clustering in alluvial basins. *Geology*, **38**, 535–536.

Hampson, G.J., **Davies, S.J.**, **Elliott, T.**, **Flint, S.S.** and **Stollhofen, H.** (1999) Incised valley fill sandstone bodies in Upper Carboniferous fluvio–deltaic strata: recognition and reservoir characterization of Southern North Sea analogues. *Geol. Soc. London Petrol. Geol. Conf. Ser.*, **5**, 771–788.

Haszeldine, R.S. and **Anderton, R.** (1980) A braidplain facies model for the Westphalian B Coal Measures of north-east England. *Nature*, **284**, 51–53.

Heckel, P.H. (1986) Sea-level curve for Pennsylvanian eustatic marine transgressive-regressive depositional cycles along midcontinent outcrop belt, North America. *Geology*, **14**, 330–334.

Heckel, P.H. (2008) Pennsylvanian cyclothems in Midcontinent North America as far-field effects of waxing and waning of Gondwana ice sheets. *Geol. Soc. Am. Spec. Pap.*, **441**, 275–289.

Heller, P.L. and **Paola, C.** (1996) Downstream changes in alluvial architecture: an exploration of controls on channel stacking patterns. *J. Sed. Res.*, **66**, 297–306.

Horne, J.C. (1978) Sedimentary responses to contemporaneous tectonism. In: *Carboniferous Depositional Environments: Eastern Kentucky and West Virginia* (Eds J.C. Horne and J.C. Ferm), pp. 27–34. University of South Carolina, Field Guide, Columbia, SC.

Jones, N.S. and **Glover, B.W.** (2005) Fluvial sandbody architecture, cyclicity and sequence stratigraphical setting – implications for hydrocarbon reservoirs: the Westphalian C and D of the Osnabrück and Ibbenbüren area, Northwest

Germany. In: *Carboniferous Hydrocarbon Geology – The Southern North Sea and Surrounding Onshore Areas* (Eds J.D. Collinson, D.J. Evans, D.W. Holliday and N.S. Jones), *Yorks. Geol. Soc. Occ. Publ.*, **7**, 57–74.

Jones, J.A. and **Hartley, A.J.** (1993) Reservoir characteristics of a braid-plain depositional system: the Upper Carboniferous Pennant Sandstone of South Wales. In: *Characterization of Fluvial and Aeolian Reservoirs* (Eds C.P. North and D.J. Prosser), *Geol. Soc. London. Spec. Publ.*, **73**, 143–156.

Jureczka, J. and **Kotas, A.** (1995) Coal Deposits – Upper Silesian Coal Basin. In: *The Carboniferous System in Poland* (Eds A. Zdanowski and H. Zakowa), pp. 164–172. Prace Panstwowego Instytutu Geologicznego, Warsaw.

Kim, W., **Sheetsz, B.A.** and **Paola, C.** (2010) Steering of experimental channels by lateral basin tilting. *Basin Res.*, **22**, 286–302.

Klein, G. and **Kupperman, J.B.** (1992) Pennsylvanian cyclothems: methods of distinguishing tectonically induced changes in sea level from climatically induced changes. *Geol. Soc. Am. Bull.*, **104**, 166–175.

Klein, G. and **Willard, D.A.** (1989) Origin of Pennsylvanian coal-bearing cyclothems of North America. *Geology*, **17**, 152–155.

Kopp, J. and **Kim, W.** (2015) The effect of lateral tectonic tilting on fluviodeltaic surficial and stratal asymmetries: experiment and theory. *Basin Res.*, 14. Online early view.

Kotas, A. (1994) Coal-bed methane potential of the Upper Silesian Coal Basin, Poland. *Pr. Panstw. Inst. Geol. Warsaw*, **142**, 81.

Kotas, A. (1995) Lithostratigraphy and sedimentologic-paleogeographic development: Upper Silesian Coal Basin. In: *The Carboniferous System of Poland* (Eds A. Zdanowski and H. Zakowa), *Pr. Panstw. Inst. Geol.*, **148**, 124–134.

Leeder, M.R. and **Gawthorpe, R.L.** (1987) Sedimentary models for extensional tilt-block/half-graben basins. In: *Continental Extensional Tectonics* (Eds M.P. Coward, J.F. Dewey and P.L. Hancock), *Geol. Soc. London. Spec. Publ.*, **28**, 139–152.

Leeder, M.R., **Mack, G.H.**, **Peakall, J.** and **Salyards, S.L.** (1996) First quantitative test of alluvial stratigraphic models: Southern Rio Grande rift, New Mexico. *Geology*, **24**, 87–90.

Mack, G.H. and **James, W.C.** (1993) Control of basin symmetry on fluvial lithofacies, Camp Rice and Palomas Formations (Plio-Pleistocene), southern Rio Grande rift, USA. In: *Alluvial Sedimentation* (Eds M. Marzo and C. Puigdefabregas), *IAS Spec. Publ.*, **17**, 439–449.

Mackey, S.D. and **Bridge, J.S.** (1995) Three-dimensional model of alluvial stratigraphy; theory and applications. *J. Sed. Res.*, **65**, 7–31.

McCabe, P.J. (1984) Depositional environments of coal and coal-bearing strata. In: *Sedimentology of Coal and Coal-bearing Sequences* (Eds R.A. Rahmani and R.M. Flores), *IAS Spec. Publ.*, **7**, 11–42.

Nadon, G.C. (1998) Magnitude and timing of peat-to-coal compaction. *Geology*, **26**, 727–730.

Paola, C. (2000) Quantitative models of sedimentary basin filling. *Sedimentology*, **47**, 121–178.

Peakall, J. (1998) Axial river evolution in response to half-graben faulting: Carson River, Nevada, U.S.A. *J. Sed. Res.*, **68**, 788–799.

Peakall, J., **Leeder, M.**, **Best, J.** and **Ashworth, P.** (2000) River response to lateral ground tilting: a synthesis and some implications for the modeling of alluvial architecture in extensional basins. *Basin Res.*, **12**, 413–424.

Rippon, J.H. (1996) Sand body orientation, palaeoslope analysis and basin-fill implications in the Westphalian A-C of Great Britain. *J. Geol. Soc. London*, **153**, 881–900.

Rygel, M.C., **Fielding, C.R.**, **Frank, T.D.** and **Birgenheier, L.P.** (2008) The magnitude of Late Paleozoic glacioeustatic fluctuations: a synthesis. *J. Sed. Res.*, **78**, 500–511.

Shanley, K.W. and **McCabe, P.J.** (1993) Alluvial architecture in a sequence stratigraphic framework: a case study from the Upper Cretaceous of southern Utah, USA. In: *The Geological Modelling of Hydrocarbon Reservoirs and Outcrop Analogues* (Eds S.S. Flint and I.D. Bryant), *IAS Spec. Publ.*, **15**, 21–56.

Straub, K.M., **Paola, C.**, **Kim, W.** and **Sheets, B.** (2013) Experimental investigation of sediment-dominated vs. tectonics-dominated sediment transport systems in subsiding basins. *J. Sed. Res.*, **83**, 1162–1180.

Van Asselen, S., **Stouthamer, E.** and **Smith, N.D.** (2010) Factors controlling peat compaction in alluvial floodplains: a case study in the Cold-Temperate Cumberland Marshes, Canada. *J. Sed. Res.*, **80**, 155–166.

Van Bergen, F., **Pagnier, H.** and **Krzystolik, P.** (2006) Field experiment of enhanced coalbed methane-CO_2 in the upper Silesian basin of Poland. *Environ. Geosci.*, **13**, 201–224.

Van Bergen, F., **Krzystolik, P.**, **van Wageningen, N.**, **Pagnier, H.**, **Jura, B.**, **Skiba, J.**, **Winthaegen, P.** and **Kobiela, Z.** (2009) Production of gas from coal seams in the Upper Silesian Coal Basin in Poland in the post-injection period of an ECBM pilot site. *Int. J. Coal Geol.*, **77**, 175–187.

Van den Belt, F.J.G. (2012) *Sedimentary Cycles in Coal and Evaporite Basins and the Reconstruction of Palaeozoic Climate*. Unpublished PhD Dissertation, University of Utrecht, 100 pp.

Weisenfluh, G.A. and **Ferm, J.C.** (1984) Geologic controls on deposition of the Pratt Seam, Black Warrior Basin, Alabama, U.S.A. In: *Sedimentology of Coal and Coal-bearing Sequences* (Eds R.A. Rahmani and R.M. Flores), *IAS Spec. Publ.*, **17**, 317–330.

Weller, J.M. (1930) Cyclical sedimentation of the Pennsylvanian period and its significance. *J. Geol.*, **38**, 97–135.

Zdanowski, A. and **Zakowa, H.** (1995) The Carboniferous System of Poland. *Pr. Panstw. Inst. Geol. Warsaw*, **148**, 215.

Ziegler, P.A. (1990) *Geological Atlas of Western and Central Europe*. Shell Internationale Petroleum Maatschappij, Den Haag, 239 pp.

